

# Flexural Behavior of a Rotating Sandwich Tapered Beam

C. L. Ko\*

Oakland University, Rochester, Michigan

Governing equations for the dynamic and flexural behavior of a rotating sandwich tapered beam with two nonsymmetrical facings are formulated by using the variational principle. Because of the asymmetric geometry and the centrifugal effects, the neutral axis does not necessarily coincide with the centroidal axis. The analysis takes this behavior into consideration and, therefore, differs from existing formulations substantially. Both the core and facings are consistently modeled as either Timoshenko beams or Euler-Bernoulli beams. The flexural behavior of tapered sandwich rotating beams with uniformly or linearly distributed loads is investigated by solving the governing equation using the finite-difference technique.

## I. Introduction

**S**ANDWICH constructions with high-strength facings and a lightweight core have been very popular in aerospace applications. Typical sandwich members used varied from structural panels in aircraft and spacecraft to the helicopter rotor blades. (See Ref. 1 for a brief overview of various applications.) An additional possible application that has not been investigated extensively is related to the construction of structural components of robots. In general, the lightweight and high-modulus characteristics of the sandwich construction normally have great advantages of high movability, power-saving, quick response time, and high strength in robotics applications.

Extensive publications have been available concerning the design and analysis of sandwich structures. References 2 and 3 are entirely devoted to this subject. Knoell and Robinson<sup>4</sup> also summarized important developments for flexural and vibration analyses of sandwich beams. To name a few, they include Hoff and Mautner,<sup>5</sup> Yu,<sup>6</sup> Mead and Markus,<sup>7</sup> Di Taranto,<sup>8</sup> Hashin,<sup>9</sup> and Krajcinovic.<sup>10</sup> In addition, Kimel et al.,<sup>11</sup> Raville et al.,<sup>12</sup> James,<sup>13</sup> Glaser,<sup>14</sup> Clary and Leadbetter,<sup>15</sup> and Bert et al.<sup>16</sup> also performed experimental measurements of natural frequencies and damping behavior of a rectangular sandwich beam. All of the analyses mentioned were primarily for a symmetrical rectangular beam without rotation. For such cases, the neutral axis was considered to be the centroidal axis of the beam. For a nonsymmetrical rotating beam, the neutral axis is no longer coincident with the centroidal axis due to the variations of axial displacement resulted from both the asymmetric tapering and centrifugal effects. Lo and Renbarger<sup>17</sup> and Boyce et al.<sup>18</sup> investigated the vibrations of uniform rotating beams without considering the effect upon the neutral axis position from the centrifugal actions. Recently, Tomar and Jain<sup>19</sup> considered thermal effect on natural frequencies of a rotating wedge-shaped uniform beam. Hoa<sup>20</sup> and Laurenson<sup>21</sup> also considered the influence of mass representation for rotating structures. However, based on the author's knowledge, the rotational effects upon the behavior of a sandwich tapered beam never have been investigated up to this date.

As it was pointed out by many investigators (see Ref. 4), the shear deformation of the core plays an important role in the flexural and dynamic behavior of a sandwich beam. Therefore, the flexural rigidity in the core and the shear deformation of the facings were neglected in many analyses.<sup>4,5,8,16</sup> For general ap-

plications, such as helicopter rotor blades, these quantities may become significant. Hence, they are included in this analysis. Similar consideration was adopted by Yu<sup>6</sup> for analysis of sandwich plates. However, the deviation of the neutral axis position from the location of the centroidal axis was not considered in his analysis.

The inertio-elastic instability of rotating uniform beams first was reported by Brunelle.<sup>22,23</sup> This instability is similar to the buckling instability, except its mechanism is due to the centrifugal force instead of a compressive force. Bisshop<sup>24</sup> later extended Brunelle's work by including the effect of Poisson's ratio to a first-order approximation. Bert<sup>25</sup> also improved the analysis and applied it to brush-type super flywheels. However, these existing analyses did not include the bending effect upon the instability phenomenon. The analysis presented in this paper yields both extensional and flexural modes of instability for a sandwich beam, which have never been reported in literature.

## II. Deformations of a Beam Element

### Timoshenko Beams

A differential element of a deformed Timoshenko beam with an undeformed length  $dx$  is shown in Fig. 1. The  $x$ -axis of the undeformed beam is positioned at a reference plane  $M_1M_2$ , and the neutral plane  $N_1N_2$  is located at  $y = \eta$ . The line normal to the neutral axis  $A_1B_1$  undergoes a rotation with an angle  $\psi$  and becomes the line  $A'_1B'_1$ . Similarly, the line  $A_2B_2$  rotates with an angle  $\psi + d\psi$  and becomes the line  $A'_2B'_2$  as a result of the deformation. The reference plane  $M_1M_2$  and a plane segment  $L_1L_2$  located at  $y$  are deformed into planes  $M'_1M'_2$  and  $L'_1L'_2$ , respectively. The arc length of the segment  $L_1L_2$  can be related to the differential arc angle as

$$L_1L_2 = (\rho_0 + y) d\theta \quad (1)$$

where  $\rho_0$  is the radius of curvature of the reference plane  $M_1M_2$ .

This differential arc angle is also related to the undeformed differential length as follows:

$$d\theta = \frac{dx}{\rho_n} \quad (2)$$

where  $\rho_n$  is the radius of curvature of the neutral plane  $N_1N_2$ , and it can be determined as

$$\rho_n = \rho_0 + \eta \quad (3)$$

Received June 8, 1987; revision received Feb. 16, 1988. Copyright © American Institute of Aeronautics and Astronautics, Inc., 1988. All rights reserved.

\*Assistant Professor, Department of Mechanical Engineering. Member AIAA.

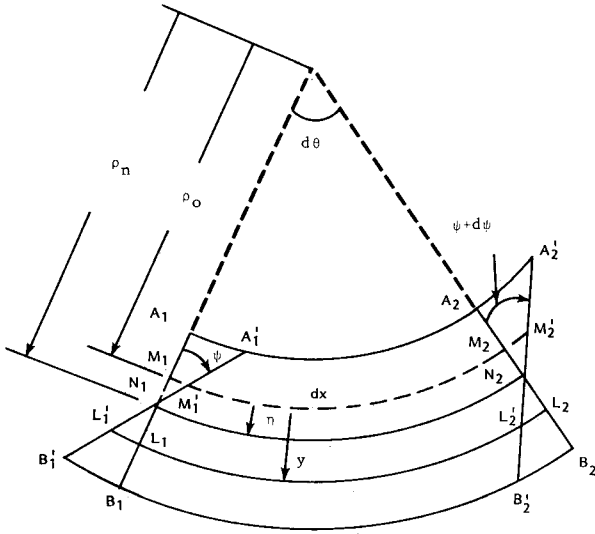


Fig. 1 Deformation of a beam element.

Substituting Eqs. (2) and (3) into Eq. (1), one obtains

$$L_1 L_2 = \left(1 - \frac{\eta}{\rho_n} + \frac{y}{\rho_n}\right) dx \quad (4)$$

The deformed arc length  $L'_1 L'_2$  can also be determined as

$$L'_1 L'_2 = L_1 L_2 - (y - \eta) \frac{\partial \psi}{\partial x} dx \quad (5)$$

The tensile strain at the location  $y$  can be evaluated as

$$\varepsilon = \frac{L'_1 L'_2 - dx}{dx} \quad (6)$$

Substituting Eqs. (4) and (5) into Eq. (6), one obtains

$$\varepsilon = (y - \eta) \left( \frac{1}{\rho_n} - \frac{\partial \psi}{\partial x} \right) \quad (7)$$

The differential axial elongation of the reference axis can also be evaluated as

$$du_0 = M'_1 M'_2 - dx \quad (8)$$

The deformed arc length of the reference axis  $M'_1 M'_2$  can be determined as

$$M'_1 M'_2 = M_1 M_2 + \eta \frac{\partial \psi}{\partial x} dx = \rho_o d\theta + \eta \frac{\partial \psi}{\partial x} dx \quad (9)$$

Substituting Eqs. (2), (3), and (9) into Eq. (8), one obtains

$$du_0 = \eta \left( \frac{\partial \psi}{\partial x} - \frac{1}{\rho_n} \right) dx \quad (10)$$

Hence, the tensile strain at the reference plane becomes

$$\varepsilon_0 = \frac{\partial u_0}{\partial x} = \eta \left( \frac{\partial \psi}{\partial x} - \frac{1}{\rho_n} \right) \quad (11)$$

Substituting Eq. (11) into Eq. (7) yields

$$\varepsilon = \frac{\partial u}{\partial x} = \frac{\partial u_0}{\partial x} + y \left( \frac{1}{\rho_n} - \frac{\partial \psi}{\partial x} \right) \quad (12)$$

If the deflection in the  $y$ -direction  $w$  is assumed to be small, then the curvature of the neutral axis can be approximated as

$$\frac{1}{\rho_n} \approx - \frac{\partial^2 w_n}{\partial x^2} \quad (13)$$

where  $w_n$  is the deflection of the neutral axis in the  $y$ -direction. The strain distribution in Eq. (12) can then be expressed as

$$\varepsilon = \frac{\partial u_0}{\partial x} - y \left( \frac{\partial \psi}{\partial x} + \frac{\partial^2 w_n}{\partial x^2} \right) \quad (14)$$

Equation (14) implies that the axial strain varies linearly with respect to  $y$ . The location of the neutral axis can be determined by imposing the condition of zero strain at  $y = \eta$  in Eq. (14) as

$$\eta = \frac{(\partial u_0 / \partial x)}{(\partial \psi / \partial x) + (\partial^2 w_n / \partial x^2)} \quad (15)$$

Equation (15) implies that the position of the neutral axis varies along the longitudinal direction of the beam unless the neutral axis coincides with the reference axis.

The axial displacement function can be obtained by integrating Eq. (14) with respect to  $x$ . In the beam theory, it is acceptable to assume that the beam element is unstrained in the  $y$ -direction, i.e., the deflection function does not vary in the  $y$ -direction. In order to be consistent with this assumption and the small-deflection theory, the higher-order integration function is neglected, and the displacement functions are approximated as

$$u = u_0 - y \left( \psi + \frac{\partial w_0}{\partial x} \right) \quad (16)$$

$$w = w_0 = w_n \quad (17)$$

Therefore, the normal and shear strains can be expressed as

$$\varepsilon = \frac{\partial u_0}{\partial x} - y \left( \frac{\partial \psi}{\partial x} + \frac{\partial^2 w_0}{\partial x^2} \right) \quad (18)$$

$$\gamma = \frac{\partial u}{\partial y} + \frac{\partial w}{\partial x} = -\psi \quad (19)$$

#### Euler-Bernoulli Beams

For an Euler-Bernoulli beam, the rotation  $\psi$  and the shear strain  $\gamma$  are neglected. Hence, Eq. (7) reduces to

$$\varepsilon = (y - \eta) / \rho_n \quad (20)$$

The tensile strain at the reference plane expressed in Eq. (11) becomes

$$\varepsilon_0 = -\eta / \rho_n \quad (21)$$

Applying the approximations of Eqs. (13) and (17), one obtains

$$\varepsilon = \frac{\partial u_0}{\partial x} - y \frac{\partial^2 w_0}{\partial x^2} \quad (22)$$

The axial displacement can be expressed as follows by neglecting higher-order functions:

$$u = u_0 - y \frac{\partial w_0}{\partial x} \quad (23)$$

### III. Formulations of the Governing Equations

The problem modeled is a cantilever rectangular sandwich beam with a fixed boundary at one end and a free boundary at the other end, as shown in Fig. 2. The depths of the core and

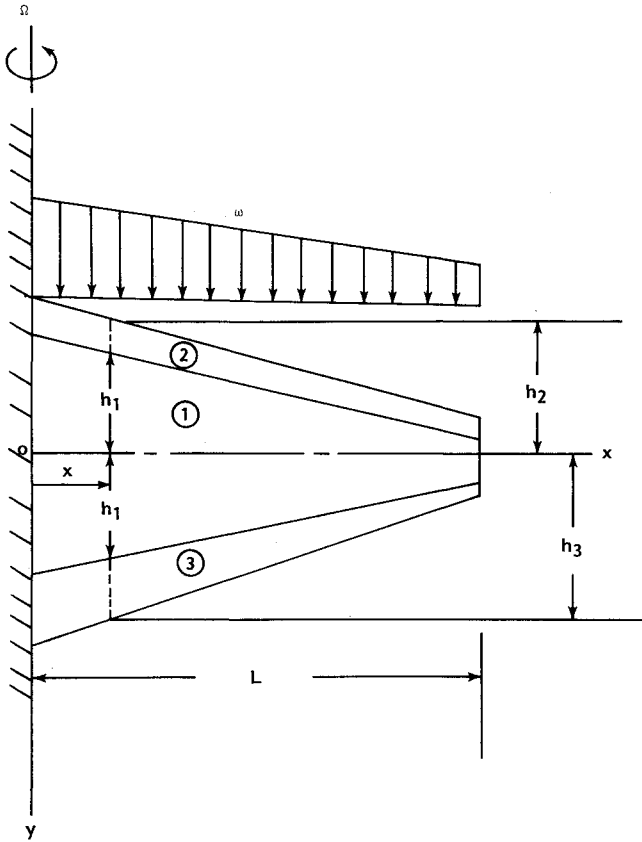


Fig. 2 A rotating sandwich cantilever beam.

facings can vary along the longitudinal axis of the beam. The origin of the Cartesian coordinate system shown is located at the center of the core at the fixed end. The half-depth of the core is  $h_1$ , and the transverse coordinates of the outer edges of the top and the bottom faces are  $-h_2$  and  $h_3$ , respectively. The length and the width of the beam are  $L$  and  $b$ , respectively. The Young's moduli of the core, the top face and the bottom face are  $E_1$ ,  $E_2$ , and  $E_3$ , respectively. In contrast, the densities of these three materials are  $\rho_1$ ,  $\rho_2$ , and  $\rho_3$ , respectively. The beam is rotating with respect to the  $y$ -axis with a constant angular speed  $\Omega$ , and the transverse component of the distributed load per unit length acting on the beam is  $\omega$ , which can be a function of both  $x$  and  $t$ . The distributed axial loads on the beam are not shown in the figure. The vibration characteristics and the flexural behavior are investigated by modeling it as either a Timoshenko beam or a Euler-Bernoulli beam with their displacement functions expressed in Eqs. (16) and (17).

Consider a point located at  $(x, y, z)$  in the undeformed beam, which is displaced to the position  $(x + u, y + w, z)$  due to deformations; the position of the point after deformation takes place can be expressed as

$$\mathbf{R} = (x + u)\hat{e}_x + (y + w)\hat{e}_y + z\hat{e}_z \quad (24)$$

Unit vectors  $\hat{e}_x$ ,  $\hat{e}_y$ , and  $\hat{e}_z$  are in  $x$ ,  $y$ , and  $z$  directions, which are the geometric axes of the beam. The angular velocity of the beam can be expressed as

$$\boldsymbol{\Omega} = -\Omega\hat{e}_y \quad (25)$$

The relative velocity of the beam at  $(x, y, z)$  with respect to the undeformed position can be determined as

$$\mathbf{v} = \frac{d\mathbf{R}}{dt} = \left(\frac{\partial u}{\partial t} - z\Omega\right)\hat{e}_x + \frac{\partial w}{\partial t}\hat{e}_y + (x + u)\Omega\hat{e}_z \quad (26)$$

Applying the variational principle for the sandwich beam with nonconservative forces, one obtains the variation of the Lagrangian as

$$\int_{t_1}^{t_2} \delta T dt - \int_{t_1}^{t_2} \delta V dt + \int_{t_1}^{t_2} \delta W dt = 0 \quad (27)$$

where  $\delta W$  is the virtual work done by the nonconservative forces applied on the beam,  $\delta T$  is the variation of total kinetic energy, and  $\delta V$  is the variation of total strain energy of the beam.

#### Timoshenko Beams

The total kinetic energy  $T$  can be determined by using Eq. (26) as

$$T = T_1 + T_2 + T_3 \quad (28)$$

where

$$T_1 \equiv \frac{1}{2} \int_0^L \int_{-b/2}^{b/2} \left[ \int_{-h_1}^{h_1} \rho_1 \left( \frac{\partial u}{\partial t} - z\Omega \right)^2 dy + \int_{-h_2}^{-h_1} \rho_2 \left( \frac{\partial u}{\partial t} - z\Omega \right)^2 dy + \int_{h_1}^{h_3} \rho_3 \left( \frac{\partial u}{\partial t} - z\Omega \right)^2 dy \right] dz dx \quad (29)$$

$$T_2 \equiv \frac{1}{2} \int_0^L \int_{-b/2}^{b/2} \left[ \int_{-h_1}^{h_1} \rho_1 \left( \frac{\partial w}{\partial t} \right)^2 dy + \int_{-h_2}^{-h_1} \rho_2 \left( \frac{\partial w}{\partial t} \right)^2 dy + \int_{h_1}^{h_3} \rho_3 \left( \frac{\partial w}{\partial t} \right)^2 dy \right] dz dx \quad (30)$$

$$T_3 \equiv \frac{1}{2} \int_0^L \int_{-b/2}^{b/2} \left[ \int_{-h_1}^{h_1} \rho_1 \Omega^2 (x + u)^2 dy + \int_{-h_2}^{-h_1} \rho_2 \Omega^2 (x + u)^2 dy + \int_{h_1}^{h_3} \rho_3 \Omega^2 (x + u)^2 dy \right] dz dx \quad (31)$$

The total strain energy  $V$  can be evaluated as

$$V = V_1 + V_2 \quad (32)$$

where

$$V_1 \equiv \frac{b}{2} \int_0^L \left[ \int_{-h_1}^{h_1} E_1 \epsilon^2 dy + \int_{-h_2}^{-h_1} E_2 \epsilon^2 dy + \int_{h_1}^{h_3} E_3 \epsilon^2 dy \right] dx \quad (33)$$

$$V_2 \equiv \frac{b}{2} \int_0^L \left[ \int_{-h_1}^{h_1} k_1 G_1 \gamma^2 dy + \int_{-h_2}^{-h_1} k_2 G_2 \gamma^2 dy + \int_{h_1}^{h_3} k_3 G_3 \gamma^2 dy \right] dx \quad (34)$$

The quantities  $k_1$ ,  $k_2$ , and  $k_3$  are the shear correction factors for the core, the top, and the bottom faces, respectively. The shear moduli for these three materials are denoted as  $G_1$ ,  $G_2$ , and  $G_3$ .

The nonconservative forces applied on the beam consist of damping forces and applied loads. Therefore, the total virtual work that results from these forces can be expressed as

$$\delta W = \delta W_{d1} + \delta W_{d2} + \delta W_p \quad (35)$$

where the virtual work due to viscous damping forces can be expressed as

$$\begin{aligned} \delta W_{d1} \equiv & - \int_0^L \int_{-b/2}^{b/2} \left[ \int_{-h_1}^{h_1} C_{x1} \left( \frac{\partial u}{\partial t} - z\Omega \right) \delta u \, dy \right. \\ & + \int_{-h_2}^{-h_1} C_{x2} \left( \frac{\partial u}{\partial t} - z\Omega \right) \delta u \, dy \\ & \left. + \int_{h_1}^{h_3} C_{x3} \left( \frac{\partial u}{\partial t} - z\Omega \right) \delta u \, dy \right] dz \, dx \quad (36a) \end{aligned}$$

$$\begin{aligned} \delta W_{d2} \equiv & -b \int_0^L \left[ \int_{-h_1}^{h_1} C_{y1} \frac{\partial w}{\partial t} \delta w \, dy \right. \\ & + \int_{-h_2}^{-h_1} C_{y2} \frac{\partial w}{\partial t} \delta w \, dy + \left. \int_{h_1}^{h_3} C_{y3} \frac{\partial w}{\partial t} \delta w \, dy \right] dx \quad (36b) \end{aligned}$$

The quantities  $C_{x1}$ ,  $C_{x2}$ , and  $C_{x3}$  are the damping coefficients for the axial vibrations, and  $C_{y1}$ ,  $C_{y2}$ , and  $C_{y3}$  are the same quantities for the transverse vibrations of the three different materials. The virtual work due to the applied loads can be expressed as

$$\delta W_p \equiv b \int_0^L [\omega(x,t) \delta w_0 + f_1(x,t) \delta u_t + f_2(x,t) \delta u_b] \, dx \quad (37)$$

where  $\omega$ ,  $f_1$ , and  $f_2$  are the distributed transverse load and the axial loads at the top and bottom faces, respectively. The axial displacement at the top and the bottom surfaces can be evaluated from Eq. (16) as

$$u_t = u_0 + h_2 \left( \psi + \frac{\partial w_0}{\partial x} \right) \quad (38)$$

$$u_b = u_0 - h_3 \left( \psi + \frac{\partial w_0}{\partial x} \right) \quad (39)$$

Applying the variational principle by substituting Eqs. (28), (32), and (35) into Eq. (27), one can obtain three simultaneous partial differential equations as

$$\begin{aligned} a_1 \frac{\partial^2 u_0}{\partial t^2} + a_8 \frac{\partial u_0}{\partial t} - a_2 \left( \frac{\partial^2 \psi}{\partial t^2} + \frac{\partial^3 w_0}{\partial x \partial t^2} \right) - a_9 \left( \frac{\partial \psi}{\partial t} + \frac{\partial^2 w_0}{\partial x \partial t} \right) \\ + \frac{\partial}{\partial x} \left[ a_5 \left( \frac{\partial \psi}{\partial x} + \frac{\partial^2 w_0}{\partial x^2} \right) - a_4 \frac{\partial u_0}{\partial x} \right] \\ + \Omega^2 \left[ a_2 \left( \psi + \frac{\partial w_0}{\partial x} \right) - a_1 (x + u_0) \right] \\ = f_1 + f_2 \quad (40) \end{aligned}$$

$$\begin{aligned} a_3 \left( \frac{\partial^2 \psi}{\partial t^2} + \frac{\partial^3 w_0}{\partial x \partial t^2} \right) + a_{10} \left( \frac{\partial \psi}{\partial t} + \frac{\partial^2 w_0}{\partial x \partial t} \right) \\ + a_7 \psi - a_2 \frac{\partial^2 u_0}{\partial t^2} - a_9 \frac{\partial u_0}{\partial t} \\ + \frac{\partial}{\partial x} \left[ a_5 \frac{\partial u_0}{\partial x} - a_6 \left( \frac{\partial \psi}{\partial x} + \frac{\partial^2 w_0}{\partial x^2} \right) \right] \\ + \Omega^2 \left[ a_2 (x + u_0) - a_3 \left( \psi + \frac{\partial w_0}{\partial x} \right) \right] \\ = f_1 h_2 - f_2 h_3 \quad (41) \end{aligned}$$

$$\begin{aligned} a_1 \frac{\partial^2 w_0}{\partial t^2} + a_{11} \frac{\partial w_0}{\partial t} + \frac{\partial}{\partial x} \\ \times \left[ a_2 \frac{\partial^2 u_0}{\partial t^2} - a_3 \left( \frac{\partial^3 w_0}{\partial x \partial t^2} + \frac{\partial^2 \psi}{\partial t^2} \right) \right] \\ + \frac{\partial^2}{\partial x^2} \left[ a_6 \left( \frac{\partial \psi}{\partial x} + \frac{\partial^2 w_0}{\partial x^2} \right) - a_5 \frac{\partial u_0}{\partial x} \right] \\ + \frac{\partial}{\partial x} \left[ a_9 \frac{\partial u_0}{\partial t} - a_{10} \left( \frac{\partial \psi}{\partial t} + \frac{\partial^2 w_0}{\partial x \partial t} \right) \right] \\ + \Omega^2 \frac{\partial}{\partial x} \left[ a_3 \left( \psi + \frac{\partial w_0}{\partial x} \right) - a_2 (x + u_0) \right] \\ = \omega + \frac{\partial}{\partial x} (f_2 h_3 - f_1 h_2) \quad (42) \end{aligned}$$

where

$$\begin{aligned} a_1 & \equiv (2\rho_1 - \rho_2 - \rho_3)h_1 + \rho_2 h_2 + \rho_3 h_3 \\ a_2 & \equiv [\rho_2(h_1^2 - h_2^2) + \rho_3(h_3^2 - h_1^2)]/2 \\ a_3 & \equiv [2\rho_1 h_1^3 + \rho_2(h_3^3 - h_1^3) + \rho_3(h_3^3 - h_1^3)]/3 \\ a_4 & \equiv (2E_1 - E_2 - E_3)h_1 + E_2 h_2 + E_3 h_3 \\ a_5 & \equiv [E_2(h_1^2 - h_2^2) + E_3(h_3^2 - h_1^2)]/2 \\ a_6 & \equiv [2E_1 h_1^3 + E_2(h_2^3 - h_1^3) + E_3(h_3^3 - h_1^3)]/3 \\ a_7 & \equiv 2k_1 G_1 h_1 + k_2 G_2 (h_2 - h_1) + k_3 G_3 (h_3 - h_1) \\ a_8 & \equiv (2C_{x1} - C_{x2} - C_{x3})h_1 + C_{x2} h_2 + C_{x3} h_3 \\ a_9 & \equiv [C_{x2}(h_1^2 - h_2^2) + C_{x3}(h_3^2 - h_1^2)]/2 \\ a_{10} & \equiv [2C_{x1} h_1^3 + C_{x2}(h_2^3 - h_1^3) + C_{x3}(h_3^3 - h_1^3)]/3 \\ a_{11} & \equiv (2C_{y1} - C_{y2} - C_{y3})h_1 + C_{y2} h_2 + C_{y3} h_3 \end{aligned}$$

In addition to the governing equations, the boundary conditions for the beam with a fixed and a free end can be derived from Eq. (32) as

1) At the fixed end ( $x = 0$ ):

$$\psi = u_0 = w_0 = \frac{\partial w_0}{\partial x} = 0 \quad (43)$$

2) At the free end ( $x = L$ ):

$$\frac{\partial \psi}{\partial x} + \frac{\partial^2 w_0}{\partial x^2} = \frac{\partial u_0}{\partial x} = 0 \quad (44)$$

$$\begin{aligned} a_2 \frac{\partial^2 u_0}{\partial t^2} - a_3 \left( \frac{\partial^2 \psi}{\partial t^2} + \frac{\partial^3 w_0}{\partial x \partial t^2} \right) \\ + \frac{\partial}{\partial x} \left[ a_6 \left( \frac{\partial \psi}{\partial x} + \frac{\partial^2 w_0}{\partial x^2} \right) - a_5 \frac{\partial u_0}{\partial x} \right] \\ + a_9 \frac{\partial u_0}{\partial t} - a_{10} \left( \frac{\partial \psi}{\partial t} + \frac{\partial^2 w_0}{\partial x \partial t} \right) \\ + \Omega^2 \left[ a_3 \left( \psi + \frac{\partial w_0}{\partial x} \right) - a_2 (L + u_0) \right] \\ + (f_1 h_2 - f_2 h_3) = 0 \quad (45) \end{aligned}$$

The governing equations, Eqs. (40–42), and the boundary conditions, Eqs. (43–45), are applicable not only for dynamic analysis but also for flexural formulations. In analysis of the flexural action, the angular speed of the rotating beam and the distributed loads are considered to be independent of time. For such a case, the dependent variables become functions of  $x$

only, and the governing equations reduce to

$$\begin{aligned} & \frac{d}{dx} \left[ a_5 \left( \frac{d\psi}{dx} + \frac{d^2 w_0}{dx^2} \right) - a_4 \frac{du_0}{dx} \right] \\ & + \Omega^2 \left[ a_2 \left( \psi + \frac{dw_0}{dx} \right) - a_1(x + u_0) \right] \\ & = f_1(x) + f_2(x) \end{aligned} \quad (46)$$

$$\begin{aligned} & \frac{d}{dx} \left[ a_5 \frac{du_0}{dx} - a_6 \left( \frac{d\psi}{dx} + \frac{d^2 w_0}{dx^2} \right) \right] \\ & + a_7 \psi + \Omega^2 \left[ a_2(x + u_0) - a_3 \left( \psi + \frac{dw_0}{dx} \right) \right] \\ & = f_1(x)h_2 - f_2(x)h_3 \end{aligned} \quad (47)$$

$$\begin{aligned} & \frac{d^2}{dx^2} \left[ a_6 \left( \frac{d\psi}{dx} + \frac{d^2 w_0}{dx^2} \right) - a_5 \frac{du_0}{dx} \right] \\ & + \Omega^2 \frac{d}{dx} \left[ a_3 \left( \psi + \frac{dw_0}{dx} \right) - a_2(x + u_0) \right] \\ & = \omega(x) + \frac{d}{dx} \left[ f_2(x)h_3 - f_1(x)h_2 \right] \end{aligned} \quad (48)$$

The boundary conditions become

1) At the fixed end ( $x = 0$ ):

$$\psi = u_0 = w_0 = \frac{dw_0}{dx} = 0 \quad (49)$$

2) At the free end ( $x = L$ ):

$$\frac{d\psi}{dx} + \frac{d^2 w_0}{dx^2} = \frac{du_0}{dx} = 0 \quad (50)$$

$$\begin{aligned} & \frac{d}{dx} \left[ a_6 \left( \frac{d\psi}{dx} + \frac{d^2 w_0}{dx^2} \right) - a_5 \frac{du_0}{dx} \right] \\ & + \Omega^2 \left[ a_3 \left( \psi + \frac{dw_0}{dx} \right) - a_2(L + u_0) \right] \\ & + [f_1(x)h_2 - f_2(x)h_3] = 0 \end{aligned} \quad (51)$$

Also, Eq. (51) can be reduced to the zero-shear condition at the free end as follows by applying Eq. (47) at  $x = L$ :

$$\psi|_{x=L} = 0 \quad (52)$$

The axial force, shear force, and bending moment per unit width of the beam at the cross section can be determined in terms of deformations as

$$H = a_4 \frac{du_0}{dx} - a_5 \left( \frac{d\psi}{dx} + \frac{d^2 w_0}{dx^2} \right) \quad (53)$$

$$V = a_7 \psi \quad (54)$$

$$M = a_5 \frac{du_0}{dx} - a_6 \left( \frac{d\psi}{dx} + \frac{d^2 w_0}{dx^2} \right) \quad (55)$$

#### Euler-Bernoulli Beams

For an Euler-Bernoulli beam, the terms that arise from the rotation of the beam element  $\psi$  are neglected. In addition, the variation of the strain energy due to shear action expressed in Eq. (34) is also discarded. Applying Eq. (27) with the reduced

expressions, one can obtain the governing equations as

$$\begin{aligned} & a_1 \frac{\partial u_0}{\partial t^2} + a_8 \frac{\partial u_0}{\partial t} - a_2 \frac{\partial^3 w_0}{\partial x \partial t^2} - a_9 \frac{\partial^2 w_0}{\partial x \partial t} \\ & + \frac{\partial}{\partial x} \left( a_5 \frac{\partial^2 w_0}{\partial x^2} - a_4 \frac{\partial u_0}{\partial x} \right) \\ & + \Omega^2 \left[ a_2 \frac{\partial w_0}{\partial x} - a_1(x + u_0) \right] = f_1 + f_2 \end{aligned} \quad (56)$$

$$\begin{aligned} & a_1 \frac{\partial^2 w_0}{\partial t^2} + a_{11} \frac{\partial w_0}{\partial t} + \frac{\partial}{\partial x} \left( a_2 \frac{\partial^2 u_0}{\partial t^2} - a_3 \frac{\partial^3 w_0}{\partial x \partial t^2} \right) \\ & + \frac{\partial^2}{\partial x^2} \left( a_6 \frac{\partial^2 w_0}{\partial x^2} - a_5 \frac{\partial u_0}{\partial x} \right) \\ & + \frac{\partial}{\partial x} \left( a_9 \frac{\partial u_0}{\partial t} - a_{10} \frac{\partial^2 w_0}{\partial x \partial t} \right) + \Omega^2 \frac{\partial}{\partial x} \\ & \times \left[ a_3 \frac{\partial w_0}{\partial x} - a_2(x + u_0) \right] \\ & = \omega + \frac{\partial}{\partial x} (f_2 h_3 - f_1 h_2) \end{aligned} \quad (57)$$

The boundary conditions become

1) At the fixed end ( $x = 0$ ):

$$u_0 = w_0 = \frac{\partial w_0}{\partial x} = 0 \quad (58)$$

2) At the free end ( $x = L$ ):

$$\frac{\partial u_0}{\partial x} = \frac{\partial^2 w_0}{\partial x^2} = 0 \quad (59)$$

$$\begin{aligned} & a_2 \frac{\partial^2 u_0}{\partial t^2} - a_3 \frac{\partial^3 w_0}{\partial x \partial t^2} + \frac{\partial}{\partial x} \left( a_6 \frac{\partial^2 w_0}{\partial x^2} - a_5 \frac{\partial u_0}{\partial x} \right) \\ & + a_9 \frac{\partial u_0}{\partial t} - a_{10} \frac{\partial^2 w_0}{\partial x \partial t} + \Omega^2 \left[ a_3 \frac{\partial w_0}{\partial x} - a_2(L + u_0) \right] \\ & = f_2 h_3 - f_1 h_2 \end{aligned} \quad (60)$$

For semistatic consideration of the flexural action only, the governing equations reduce to

$$\begin{aligned} & \frac{d}{dx} \left( a_5 \frac{d^2 w_0}{dx^2} - a_4 \frac{du_0}{dx} \right) + \\ & \Omega^2 \left[ a_2 \frac{dw_0}{dx} - a_1(u_0 + x) \right] \\ & = f_1 + f_2 \end{aligned} \quad (61)$$

$$\begin{aligned} & \frac{d^2}{dx^2} \left( a_6 \frac{d^2 w_0}{dx^2} - a_5 \frac{du_0}{dx} \right) + \Omega^2 \frac{d}{dx} \left[ a_3 \frac{dw_0}{dx} - a_2(u_0 + x) \right] \\ & = \omega + \frac{d}{dx} (f_2 h_3 - f_1 h_2) \end{aligned} \quad (62)$$

The boundary condition expressed in Eq. (60) becomes

$$\begin{aligned} & \frac{d}{dx} \left( a_6 \frac{d^2 w_0}{dx^2} - a_5 \frac{du_0}{dx} \right) + \Omega^2 \left[ a_3 \frac{dw_0}{dx} - a_2(u_0 + L) \right] \\ & = f_2 h_3 - f_1 h_2 \end{aligned} \quad (63)$$

The axial force, bending moment, and shear force per unit width of beam can be determined as

$$H = a_4 \frac{du_0}{dx} - a_5 \frac{d^2 w_0}{dx^2} \quad (64)$$

$$M = a_5 \frac{du_0}{dx} - a_6 \frac{d^2 w_0}{dx^2} \quad (65)$$

$$V = \frac{dM}{dx} = \frac{d}{dx} \left( a_5 \frac{du_0}{dx} - a_6 \frac{d^2 w_0}{dx^2} \right) \quad (66)$$

#### IV. Flexural Analysis for a Symmetric Rectangular Sandwich Beam With a Uniformly Distributed Load

For the case of a rectangular sandwich beam, the depths of the core and the facings are constant. Hence, the coefficients  $a$  in the governing equations and the boundary conditions are independent of  $x$ . In addition, the coefficients  $a_2$  and  $a_5$  vanish, due to symmetry in material properties and dimensions of both facings. Only a uniformly distributed load  $\omega_0$  is considered for its mathematical simplicity. However, other types of loading can be easily implemented by following the same procedures in the analysis.

The reactions at the fixed end can be incorporated into total equivalent distributed loads as follows by expressing them in terms of singularity functions<sup>26</sup>:

$$\omega = \omega_0 \langle x - 0 \rangle^0 - V_0 \langle x - 0 \rangle^{-1} + M_0 \langle x - 0 \rangle^{-2} \quad (67)$$

where  $V_0$  and  $M_0$  are the shear force and bending moment per unit width of the beam at the fixed end, respectively. The uniformly distributed load per unit width of the beam is  $\omega_0$ .

##### Timoshenko Beam

Combining Eqs. (47) and (48), one can obtain the following relation:

$$\frac{d\psi}{dx} = \frac{\omega}{a_7} \quad (68)$$

Since  $\psi$  vanishes at the fixed end, Eq. (68) can be integrated with respect to  $x$  from 0 to  $x$  to determine the angle of rotation for a uniformly distributed load  $\omega$  as

$$\psi = \frac{\omega_0}{a_7} \langle x - 0 \rangle^1 - \frac{V_0}{a_7} \langle x - 0 \rangle^0 + \frac{M_0}{a_7} \langle x - 0 \rangle^{-1} \quad (69)$$

Using Eq. (69) and also eliminating  $a_2$  and  $a_5$  from Eqs. (46) and (47), one obtains the governing equations as

$$\frac{d^2 u_0}{dx^2} + \beta^2 u_0 = -\beta^2 x \quad (70)$$

$$\frac{d^4 w_0}{dx^4} + \alpha^2 \frac{d^2 w_0}{dx^2} = \frac{\omega}{a_6} - \frac{a_3 \Omega^2 \omega}{a_7 a_6} - \frac{1}{a_7} \frac{d^2 \omega}{dx^2} \quad (71)$$

where

$$\alpha^2 \equiv a_3 \Omega^2 / a_6, \quad \beta^2 \equiv a_1 \Omega^2 / a_4$$

The boundary conditions at  $x = L$  can be obtained as follows by simplifying Eqs. (55) and (51):

$$\left. \frac{du_0}{dx} \right|_{x=L} = 0 \quad (72)$$

$$\left. \frac{d^2 w_0}{dx^2} \right|_{x=L} = -\frac{\omega}{a_7} \quad (73)$$

$$\left. \frac{d^3 w_0}{dx^3} \right|_{x=L} + \alpha^2 \left. \frac{dw_0}{dx} \right|_{x=L} = 0 \quad (74)$$

The solutions of Eqs. (68) and (69), which satisfy boundary conditions in Eqs. (72–74) and (49), can be determined as

$$u_0 = \frac{\sin \beta x}{\beta \cos \beta L} - x \quad (75)$$

$$w_0 = \frac{\omega_0 L}{a_3 \Omega^2 \alpha} \left[ \tan \alpha L (1 - \cos \alpha x) + \sin \alpha x + \left( \frac{\cos \alpha x - 1}{\alpha L \cos \alpha L} \right) + \frac{\alpha x^2}{2L} - \alpha x \right] - \frac{\omega_0 L}{a_7 \alpha} \times \left[ \tan \alpha L (1 - \cos \alpha x) + \sin \alpha x + \frac{\alpha x^2}{2L} - \alpha x \right] \quad (76)$$

It is obvious that the beam becomes unstable if either of the following conditions exist:

$$\cos \alpha L = 0 \quad (77)$$

$$\cos \beta L = 0 \quad (78)$$

The critical angular speeds of rotation can be determined as

$$\Omega = \pi(n - \frac{1}{2}) \sqrt{a_4 / a_1 L^2} \quad (79)$$

and

$$\Omega = \pi(n - \frac{1}{2}) \sqrt{a_6 / a_3 L^2} \quad (80)$$

where  $n$  can be any positive integer.

The instability is similar to the case of buckling, except that the mechanism is a result of the centrifugal force instead of a compressive force. It was first reported by Brunelle<sup>22</sup> as the inertio-elastic instability.

For a homogeneous rectangular beam that has a width  $b$ , a cross-sectional area  $A$ , and a moment of inertia  $I$ , the displacements at the free end can be determined as

$$u_0 = \frac{1}{\alpha} \tan \alpha L - L \quad (81)$$

$$w_0 = \frac{b \omega_0 L}{\rho \Omega^3 I} \sqrt{\frac{E}{\rho}} \left( \tan \alpha L + \frac{1}{\alpha L} - \frac{1}{\alpha L \cos \alpha L} - \frac{\alpha L}{2} \right) - \frac{b \omega_0 L}{k G A \Omega} \sqrt{\frac{E}{\rho}} \left( \tan \alpha L - \frac{\alpha L}{2} \right) \quad (82)$$

where  $\alpha \equiv \Omega \sqrt{\rho / E}$ . The Young's modulus, shear modulus, and the density of the beam are denoted as  $E$ ,  $G$ , and  $\rho$ , respectively. The critical angular speed expressed in Eqs. (79) and (80) becomes

$$\Omega = \pi(n - \frac{1}{2}) \sqrt{E / \rho L^2} \quad (83)$$

For a homogeneous cantilever rectangular beam subjected to uniformly distributed load without rotation, the deflection can be determined as follows by solving Eq. (71) to satisfy Eqs. (73) and (74) with  $\alpha$  and  $\Omega$  being zero:

$$w_0 = (b \omega_0 / 24 E I) (x^4 - 4 L x^3 + 6 L^2 x^2) - (b \omega_0 x^2 / 2 k G A) \quad (84)$$

The deflection at the free end can be determined as

$$w_0 = (b \omega_0 L^4 / 8 E I) - (b \omega_0 L^2 / 2 k G A) \quad (85)$$

##### Euler-Bernoulli Beams

For rectangular sandwich beams with uniformly distributed loads only, Eq. (61) reduces to Eq. (70), and Eq. (62) becomes

$$\frac{d^4 w_0}{dx^4} + \alpha^2 \frac{d^2 w_0}{dx^2} = \frac{\omega}{a_6} \quad (86)$$

The boundary condition at  $x = L$  expressed in Eq. (71) becomes

$$\frac{d^3 w_0}{dx^3} + \alpha^2 \frac{dw_0}{dx} = 0 \quad (87)$$

The solution for the axial displacement  $u_0$  is expressed in Eq. (75), and the deflection can be determined as

$$w_0 = \frac{\omega_0 L}{a_3 \Omega^2 \alpha} \left[ \tan \alpha L (1 - \cos \alpha x) + \sin \alpha x + \frac{(\cos \alpha x - 1)}{\alpha L \cos \alpha L} + \frac{\alpha^2 x}{2L} - \alpha x \right] \quad (88)$$

Again, the beam becomes unstable if the condition in either Eq. (77) or Eq. (78) exists.

The deflection at the free end for a homogeneous rectangular beam can be determined as

$$w_0 = \frac{b \omega_0 L}{\rho \Omega^3 I} \sqrt{\frac{E}{\rho}} \left( \tan \alpha L + \frac{1}{\alpha L} - \frac{1}{\alpha L \cos \alpha L} - \frac{\alpha L}{2} \right) \quad (89)$$

For the case of a homogeneous rectangular beam without rotation, Eqs. (86) and (87) reduce to the classical beam equation<sup>27</sup> and the boundary condition for zero shear at the free end as

$$\frac{d^4 w_0}{dx^4} = \frac{\omega b}{EI} \quad (90)$$

$$\left. \frac{d^3 w_0}{dx^3} \right|_{x=L} = 0 \quad (91)$$

The solution can be obtained as

$$w_0 = \frac{b \omega_0 x^2}{24EI} (x^2 - 4Lx + 6L^2) \quad (92)$$

## V. Flexural Analysis for a Tapered Rotating Sandwich Beam

Consider a tapered sandwich beam with the dimensions of the core and facings varying linearly with respect to its longitudinal axis from  $h_{10}$ ,  $h_{20}$ , and  $h_{30}$  of the fixed end ( $x = 0$ ) to  $h_{1L}$ ,  $h_{2L}$ , and  $h_{3L}$  at the free end ( $x = L$ ) as

$$h_1 = h_{10} - s_1 x, \quad h_2 = h_{20} - s_2 x, \quad h_3 = h_{30} - s_3 x \quad (93)$$

where

$$s_1 \equiv (h_{10} - h_{1L})/L, \quad s_2 \equiv (h_{20} - h_{2L})/L, \quad s_3 \equiv (h_{30} - h_{3L})/L$$

Using singularity functions, one can incorporate different types of loads into equivalent distributed loads. If the weight of the beam is the only external load, the distributed loads can be expressed as

$$\omega(x) = \omega_0 \langle x - 0 \rangle^0 - [(\omega_0 - \omega_L)/L] \langle x - 0 \rangle^1 - V_0 \langle x - 0 \rangle^{-1} + M_0 \langle x - 0 \rangle^{-2} \quad (94)$$

where  $V_0$  and  $M_0$  are shear and moment reactions at the fixed end, respectively. The linearly distributed loads at  $x = 0$  and  $x = L$  are denoted by  $\omega_0$  and  $\omega_L$ , respectively. The coefficients

of the governing equations can be evaluated as

$$\begin{aligned} a_1 &= c_1 - b_1 x & a_2 &= c_2 - d_1 x + b_2 x^2 \\ a_3 &= c_3 - d_2 x + d_3 x^2 - b_3 x^3 & a_4 &= c_4 - b_4 x \\ a_5 &= c_5 - d_4 x + b_5 x^2 & a_6 &= c_6 - d_5 x + d_6 x^2 - b_6 x^3 \\ a_7 &= c_7 - b_7 x & \alpha_1 &= d_5 - 2d_6 x + 3b_6 x^2 \\ \alpha_2 &= d_2 - 2d_3 x + 3b_3 x^2 & \alpha_3 &= 2b_5 x - d_4 \\ \alpha_4 &= 2b_2 x - d_1 & \alpha_5 &= 3b_6 x - d_6 \end{aligned} \quad (95)$$

where

$$\begin{aligned} b_1 &\equiv (2\rho_1 - \rho_2 - \rho_3)s_1 + \rho_2 s_2 + \rho_3 s_3 \\ b_2 &\equiv [\rho_2(s_1^2 - s_2^2) + \rho_3(s_3^2 - s_1^2)]/2 \\ b_3 &\equiv [(2\rho_1 - \rho_2 - \rho_3)s_1^3 + \rho_2 s_2^3 + \rho_3 s_3^3]/3 \\ b_4 &\equiv (2E_1 - E_2 - E_3)s_1 + E_2 s_2 + E_3 s_3 \\ b_5 &\equiv [E_2(s_1^2 - s_2^2) + E_3(s_3^2 - s_1^2)]/2 \\ b_6 &\equiv [(2E_1 - E_2 - E_3)s_1^3 + E_2 s_2^3 + E_3 s_3^3]/3 \\ b_7 &\equiv 2k_1 G_1 s_1 + k_2 G_2 (s_2 - s_1) + k_3 G_3 (s_3 - s_1) \\ c_1 &\equiv (2\rho_1 - \rho_2 - \rho_3)h_{10} + \rho_2 h_{20} + \rho_3 h_{30} \\ c_2 &\equiv [\rho_2(h_{10}^2 - h_{20}^2) + \rho_3(h_{30}^2 - h_{10}^2)]/2 \\ c_3 &\equiv [(2\rho_1 - \rho_2 - \rho_3)h_{10}^3 + \rho_2 h_{20}^3 + \rho_3 h_{30}^3]/3 \\ c_4 &\equiv (2E_1 - E_2 - E_3)h_{10} + E_2 h_{20} + E_3 h_{30} \\ c_5 &\equiv [E_2(h_{10}^2 - h_{20}^2) + E_3(h_{30}^2 - h_{10}^2)]/2 \\ c_6 &\equiv [(2E_1 - E_2 - E_3)h_{10}^3 + E_2 h_{20}^3 + E_3 h_{30}^3]/3 \\ c_7 &\equiv 2k_1 G_1 h_{10} + k_2 G_2 (h_{20} - h_{10}) + k_3 G_3 (h_{30} - h_{10}) \\ d_1 &\equiv \rho_2 (s_1 h_{10} - s_2 h_{20}) + \rho_3 (s_3 h_{30} - s_1 h_{10}) \\ d_2 &\equiv (2\rho_1 - \rho_2 - \rho_3)s_1 h_{10}^2 + \rho_2 s_2 h_{20}^2 + \rho_3 s_3 h_{30}^2 \\ d_3 &\equiv (2\rho_1 - \rho_2 - \rho_3)s_1^2 h_{10} + \rho_2 s_2^2 h_{20} + \rho_3 s_3^2 h_{30} \\ d_4 &\equiv E_2 (s_1 h_{10} - s_2 h_{20}) + E_3 (s_3 h_{30} - s_1 h_{10}) \\ d_5 &\equiv (2E_1 - E_2 - E_3)s_1 h_{10}^2 + E_2 s_2 h_{20}^2 + E_3 s_3 h_{30}^2 \\ d_6 &\equiv (2E_1 - E_2 - E_3)s_1^2 h_{10} + E_2 s_2^2 h_{20} + E_3 s_3^2 h_{30} \end{aligned}$$

### Timoshenko Beams

The governing equations, Eqs. (46–48), can be simplified as follows by eliminating the function  $\psi$ :

$$\begin{aligned} -a_4 \frac{d^2 u_0}{dx^2} + b_4 \frac{du_0}{dx} - a_1 \Omega^2 u_0 + a_5 \frac{d^3 w_0}{dx^3} + \alpha_3 \frac{d^2 w_0}{dx^2} \\ + a_2 \Omega^2 \frac{dw_0}{dx} = f_1 + f_2 + \Omega^2 a_1 x - \frac{a_5}{a_7} \\ \times \left[ \frac{d\omega}{dx} + \frac{2b_7}{a_7} \omega(x) + \frac{2b_7^2}{a_7^2} F(x) \right] - \frac{\Omega^2 a^2}{a_7} F(x) \\ - \frac{\alpha_3}{a_7} \left[ \omega(x) + \frac{b_7}{a_7} F(x) \right] \end{aligned} \quad (96)$$

$$\begin{aligned}
& -2(\alpha_3 a_4 + b_4 a_5) \frac{d^2 u_0}{dx^2} + [\Omega^2(a_1 a_5 - a_2 a_4) - 2b_5 a_4] \frac{du_0}{dx} \\
& - (\alpha_4 a_4 + b_1 a_5) \Omega^2 u_0 + (a_4 a_6 - a_5^2) \frac{d^4 w_0}{dx^4} \\
& - 2(\alpha_1 a_4 + \alpha_3 a_5) \frac{d^3 w_0}{dx^3} + [\Omega^2(a_3 a_4 - a_2 a_5) \\
& - 2(\alpha_5 a_4 + b_5 a_5)] \frac{d^2 w_0}{dx^2} - \Omega^2(\alpha_2 a_4 + \alpha_4 a_5) \frac{dw_0}{dx} \\
& = a_4 f_1 s_2 - a_4 f_2 s_3 + \frac{df_2}{dx} (a_4 h_3 - a_5) - \frac{df_1}{dx} (a_4 h_2 + a_5) \\
& + (a_2 a_4 - a_1 a_5) \Omega^2 + (\alpha_4 a_4 + b_1 a_5) x \Omega^2 + \frac{1}{a_7} \frac{d^2 \omega}{dx^2} \\
& \times (a_5^2 - a_4 a_6) + \frac{1}{a_7} \frac{d\omega}{dx} \left[ 2(\alpha_1 a_4 + \alpha_3 a_5) + \frac{3b_7}{a_7} (a_5^2 - a_4 a_6) \right] \\
& + \omega \left[ a_4 + \frac{2}{a_7} (\alpha_5 a_4 + b_5 a_5) + \frac{\Omega^2}{a_7} (a_2 a_5 - a_3 a_4) \right. \\
& \left. + \frac{4b_7}{a_7^2} (\alpha_1 a_4 + \alpha_3 a_5) + \frac{6b_7^2}{a_7^3} (a_5^2 - a_4 a_6) \right] + \frac{F}{a_7} \\
& \times \left[ \frac{6b_7^3}{a_7^3} (a_5^2 - a_4 a_6) + \frac{4b_7^2}{a_7^2} (\alpha_1 a_4 + \alpha_3 a_5) + \frac{2b_7}{a_7} (a_4 \alpha_5 + a_5 b_5) \right. \\
& \left. + \frac{b_7}{a_7} \Omega^2 (a_2 a_5 - a_3 a_4) + \Omega^2 (\alpha_2 a_4 + \alpha_4 a_5) \right] \quad (97)
\end{aligned}$$

$$\psi = \frac{F(x)}{a_7} \quad (98)$$

where

$$F(x) \equiv \int_0^x \omega(\xi) d\xi$$

Similarly, the boundary conditions shown in Eqs. (50) and (51) can be reduced to

$$\left[ \frac{d^2 w_0}{dx^2} + \frac{\omega}{a_7} \right]_{x=L} = 0 \quad (99)$$

$$\begin{aligned}
& \left[ a_6 \frac{d^3 w_0}{dx^3} - \alpha_1 \frac{d^2 w_0}{dx^2} + \Omega^2 a_3 \frac{dw_0}{dx} - a_5 \frac{d^2 u_0}{dx^2} - \Omega^2 a_2 (u_0 + L) \right. \\
& \left. + f_1 h_{2L} - f_2 h_{3L} + \frac{a_6}{a_7} \left( \frac{d\omega}{dx} + \frac{2b_7}{a_7} \omega \right) - \frac{\alpha_1 \omega}{a_7} \right]_{x=L} = 0 \quad (100)
\end{aligned}$$

$$F|_{x=L} = 0 \quad (101)$$

Numerical techniques can be employed to solve the governing equations, Eqs. (96–98), by incorporating the boundary conditions expressed in Eqs. (49), (50), (99), (100), and (101).

#### Euler-Bernoulli Beams

The governing equations, Eqs. (61) and (62), can be manipulated into

$$\begin{aligned}
& a_5 \frac{d^3 w_0}{dx^3} + \alpha_3 \frac{d^2 w_0}{dx^2} + \Omega^2 a_2 \frac{dw_0}{dx} + a_4 \frac{d^2 u_0}{dx^2} + b_4 \frac{du_0}{dx} \\
& - a_1 \Omega^2 u_0 = f_1 + f_2 + a_1 \Omega^2 x \quad (102)
\end{aligned}$$

$$\begin{aligned}
& (a_4 a_6 - a_5^2) \frac{d^4 w_0}{dx^4} - 2(a_4 \alpha_1 + a_5 \alpha_3) \frac{d^3 w_0}{dx^3} \\
& - [2(a_4 \alpha_5 + b_5 a_5) + \Omega^2(a_2 a_5 - a_3 a_4)] \frac{d^2 w_0}{dx^2} \\
& - \Omega^2(a_4 \alpha_2 + a_5 \alpha_4) \frac{dw_0}{dx} - 2(a_4 \alpha_3 + b_4 a_5) \frac{d^2 u_0}{dx^2} \\
& - [2b_5 a_4 + \Omega^2(a_2 a_4 + a_1 a_5)] \frac{du_0}{dx} - \Omega^2(a_4 a_4 + b_1 a_5) u_0 \\
& = \Omega^2(a_2 a_4 - a_1 a_5 + b_1 a_5 x + a_4 \alpha_4 x) + a_4 \omega + a_4 s_2 f_1 \\
& - a_4 s_3 f_2 + \frac{df_2}{dx} (h_3 a_4 - a_5) - \frac{df_1}{dx} (h_2 a_4 + a_5) \quad (103)
\end{aligned}$$

The boundary condition in Eq. (63) at the free end can be expressed as

$$\begin{aligned}
& \left[ a_6 \frac{d^3 w_0}{dx^3} + \Omega^2 a_3 \frac{dw_0}{dx} - a_5 \frac{d^2 u_0}{dx^2} - \Omega^2 a_2 u_0 \right]_{x=L} \\
& = [\Omega^2 a_2 L + f_2 h_{3L} - f_1 h_{2L}]_{x=L} \quad (104)
\end{aligned}$$

Boundary conditions in Eqs. (58) and (59) should also be applied to obtain numerical solutions.

#### VI. Numerical Examples

Three cantilever sandwich rotating beams are considered for numerical computations: a rectangular beam (beam A), a symmetrically tapered beam (beam B), and a nonsymmetrically tapered beam (beam C). Aluminum core with steel facings are modeled for the sandwich construction. Hence, the material properties are selected as

$$E_1 = 6.89 \times 10^{10} \text{ Pa } (10 \times 10^6 \text{ psi})$$

$$E_2 = E_3 = 2.07 \times 10^{11} \text{ Pa } (30 \times 10^6 \text{ psi})$$

$$G_1 = 2.62 \times 10^{10} \text{ Pa } (3.80 \times 10^6 \text{ psi})$$

$$G_2 = G_3 = 8.00 \times 10^{10} \text{ Pa } (11.5 \times 10^6 \text{ psi})$$

$$\rho_1 = 2710 \text{ kg/m}^3 \text{ (169 lbf/ft}^3\text{)}$$

$$\rho_2 = \rho_3 = 7850 \text{ kg/m}^3 \text{ (490 lbf/ft}^3\text{)}$$

The shear correction factors are chosen to be 0.850 for both materials by following Cowper's formulation<sup>28</sup> for rectangular cross sections. The beam lengths are selected as 3.05 m (10 ft) for all three beams. The half-thickness of the core  $h_1$  is chosen to be 0.0762 m (3 in.), and a uniform thickness of 0.0508 m (2 in.) is selected for both facings of beam A. The core thickness of beams B and C are tapered from 0.0762 m (3 in.) at the fixed end to 0.0254 m (1 in.) at the free end. Both facings of these beams have uniform thickness. Beam B has a symmetric geometry with the same facing thickness as those of beam A. The thickness of the bottom facing of beam C is changed to 0.0762 m (3 in.) to make the beam become nonsymmetrical. The loadings considered for all three beams are their weights only. Hence, beam A has a uniformly distributed transverse load, and beams B and C have linearly distributed loads.

Governing equations for both Timoshenko's and Euler-Bernoulli's models were solved by the finite-difference method (FDM). All three beams were divided into 50 equally spaced segments in the finite-difference computations. Table 1 shows the comparisons of axial and transverse displacements at the free end of beam A. Since the beam had a uniform cross section, exact solutions (ES) of the governing equations can be determined by Eqs. (75), (76), and (88). Results obtained by FDM are in good agreement with exact solutions. Both Timoshenko's beam model (TBM) and Euler-Bernoulli's model



**Table 1** Comparison of axial displacements ( $u_0$ ) and deflections ( $w_0$ ) at the free end ( $x = L$ ) of the rectangular beam (beam A) at various rotating speeds ( $\Omega$ )

$\Omega$ (rpm)	$u_0(L)$ (cm)		$w_0(L)$ (cm)			
	TBM and EBM		TBM		EBM	
	ES	FDM	ES	FDM	ES	FDM
0	0	0	0.05250	0.05252	0.05304	0.05306
100	0.00398	0.00398	0.05250	0.05252	0.05304	0.05306
300	0.03580	0.03580	0.05251	0.05253	0.05305	0.05307
500	0.09948	0.09948	0.05252	0.05254	0.05306	0.05308
1000	0.3984	0.3984	0.05258	0.05260	0.05312	0.05314
2000	1.601	1.601	0.05282	0.05284	0.05336	0.05338
3000	3.631	3.631	0.05322	0.05324	0.05377	0.05379
5000	10.35	10.35	0.05455	0.05457	0.05512	0.05514

**Table 2** Comparison of maximum flexural stresses near the fixed end of the rectangular beam (beam A) at various rotating speeds ( $\Omega$ ) (results calculated by TBM and EBM are identical)

$\Omega$ (rpm)	Maximum flexural stresses (MPa)							
	Core top		Core bottom		Top Facing		Bottom Facing	
	FDM $x = 61$ mm	ES $x = 0$	FDM $x = 61$ mm	ES $x = 0$	FDM $x = 61$ mm	ES $x = 0$	FDM $x = 61$ mm	ES $x = 0$
0	1.152	1.120	-1.152	-1.120	5.761	5.999	-5.761	-5.999
100	2.501	2.549	0.1966	0.1496	9.808	10.05	-1.715	-1.951
300	13.29	13.35	10.99	10.95	42.19	42.44	30.66	30.44
500	34.89	34.95	32.58	32.55	107.0	107.3	95.44	95.25
1000	136.3	136.4	134.0	134.0	411.1	411.5	399.6	399.5
2000	544.2	544.5	541.9	542.1	1635	1636	1624	1624
3000	1233	1234	1231	1231	3702	3704	3690	3692
5000	3517	3518	3514	3516	10550	10560	10540	10540

**Table 3** Axial displacements  $u_0$  and deflections  $w_0$  at the free ends of beams B and C calculated by the finite-difference method at various rotating speeds ( $\Omega$ )

$\Omega$ (rpm)	Beam B			Beam C			
	$u_0(L)$ (cm)	$w_0(L)$ (cm)		$u_0(L)$ (cm)	$w_0(L)$ (cm)		
	TBM and EBM	TBM	EBM	TBM	EBM	TBM	EBM
0	0	0.0563	0.0568	0.000512	0.000426	0.0592	0.0487
100	0.00361	0.0563	0.0568	0.00420	0.00410	0.0623	0.0505
300	0.0325	0.0563	0.0568	0.0327	0.0335	0.0869	0.0651
500	0.0902	0.0563	0.0568	0.0926	0.0923	0.1360	0.0942
1000	0.361	0.0564	0.0568	0.369	0.368	0.367	0.231
2000	1.45	0.0565	0.0570	1.483	1.478	1.297	0.783
3000	3.29	0.0568	0.0573	3.36	3.35	2.87	1.72
5000	9.35	0.0576	0.0581	9.55	9.53	8.12	4.88

(EBM) predict the same axial displacements. However, the deflections calculated by EBM are slightly greater than those calculated by TBM. The smallest value of unstable rotating speeds of this beam was estimated to be about 25,200 rpm by using Eqs. (79) and (80). Comparisons of maximum flexural stresses of the core and both facings near the fixed end of this beam are shown in Table 2. Again, results calculated by both ES and FDM are in reasonable agreement. The stresses predicted by ES are the actual stress at the fixed end, whereas those calculated by FDM are the stresses at the station located at 0.061 m from the fixed end. Therefore, it is reasonable to observe that the FDM yields slightly smaller values than those

determined by ES. Both TBM and EBM yield identical values of stresses for this case. Because of the centrifugal effect, stress distributions are not symmetric except in the case with no rotation. The top portion of the beam is under tension, and the bottom portion is under compression with negative tensile stresses for this case. The neutral axis is fixed at the centroidal axis as a result of zero displacement along this axis. For a rotating beam, the neutral axis varies its position along the beam. It moves toward the bottom edge of the beam as the distance away from the fixed end and the rotating speed increase. It is obvious from the results that the maximum stresses exceed the yield strengths of both materials when the rotating

**Table 4** Maximum flexural stresses in beam B calculated by using either Timoshenko beam model or Euler-Bernoulli beam model for various rotating speeds ( $\Omega$ )

$\Omega$ (rpm)	Maximum flexural stresses (MPa)			
	Core top	Core bottom	Top facing	Bottom facing
0	0.984	-0.984	4.95	-4.95
100	2.13	0.165	8.40	-1.50
300	11.3	9.36	36.0	26.1
500	29.7	27.8	91.2	81.3
1000	116	114	350	340
2000	463	463	1392	1382
3000	1049	1047	3150	3140
5000	2984	2982	8954	8944

**Table 5** Maximum flexural stresses in beam C calculated by the finite-difference method at  $x = 61$  mm near the fixed end for various rotating speeds ( $\Omega$ )

$\Omega$ (rpm)	Maximum flexural stresses (MPa)							
	Core top		Core bottom		Top facing		Bottom facing	
	TBM	EBM	TBM	EBM	TBM	EBM	TBM	EBM
0	1.45	1.09	-0.841	-0.633	6.65	5.01	-6.00	-4.51
100	2.69	2.30	0.296	0.523	10.49	8.69	-2.75	-1.13
300	12.6	12.0	9.39	9.77	41.7	38.2	23.3	26.0
500	32.2	31.3	27.6	28.2	102.5	97.1	75.9	80.2
1000	126	122	113	115	391	374	320	335
2000	501	488	457	465	1550	1488	1302	1358
3000	1135	1104	1036	1053	3505	3366	2958	3084
5000	3229	3144	2951	3000	9968	9577	8430	8782

speed reaches 1000 rpm, which is still considerably less than the unstable rotating speed. Therefore, dynamic instability will not be a dominant mode of failure.

Table 3 shows the comparisons of maximum displacements at the free ends of beam B and beam C calculated by FDM. Results predicted by both TBM and EBM are in good agreement for the symmetric beam (beam B). For the nonsymmetrically tapered beam (beam C), TBM predicts larger deflections than those calculated by EBM. The governing equations include nonzero terms of  $a_2$  and  $a_3$  for the nonsymmetrical case, and their effects contribute to the discrepancy between results calculated by these two models. The axial displacement at the central axis of the cord of beam C is not zero, even when no rotation occurs. This is because the neutral axis is not located at that particular point due to the nonsymmetrical geometry. The results also show that beam C has larger displacement than those of beam B. This is reasonable because beam C is heavier than beam B. The maximum stresses in these two beams calculated by FDM at the location 0.061 m away from the fixed end are shown in Table 4 and Table 5, respectively. Both TBM and EBM yield identical values for the symmetric case (beam B). For the nonsymmetrical case (beam C), results predicted by these two models are also in reasonable agreement.

## VII. Conclusion

The governing equations for the vibration and flexural behavior of a rotating sandwich beam were derived by including the effect of variations of the neutral axis position. Results obtained by flexural analysis indicate that this effect played an important role in determining the characteristics of a rotating beam or a nonsymmetric sandwich beam. Therefore, neglecting this effect may produce inaccurate results.

## Acknowledgments

This work is supported by a research excellence and economic development fund provided by the state of Michigan. The author would also like to express his gratitude to Professor Charles W. Bert of the University of Oklahoma for his helpful discussions.

## References

- <sup>1</sup>Bert, C. W., "Analysis of Plates," *Composite Materials, Structural Design and Analysis, Part I*, Vol. 7, edited by C. C. Chamis, Academic, New York, 1974, Chap. 4, pp. 194-198.
- <sup>2</sup>*Structural Sandwich Composites*, Military Handbook 23A, Department of Defense, U.S. Govt. Printing Office, Washington, DC, 1968.
- <sup>3</sup>Plantema, F. J., *Sandwich Construction*, Wiley, New York, 1966.
- <sup>4</sup>Knoell, A. C. and Robinson, E. Y., "Truss, Beam, Frame, and Membrane Components," *Composite Materials, Structural Design and Analysis, Part I*, Vol. 7, edited by C. C. Chamis, Academic, New York, 1974, Chap. 3, pp. 137-139.
- <sup>5</sup>Hoff, N. J. and Mautner, S. E., "Bending and Buckling of Sandwich Beams," *Journal of Aeronautical Science*, Vol. 15, Dec. 1948, pp. 707-720.
- <sup>6</sup>Yu, Y.-Y., "A New Theory of Elastic Sandwich Plates—One-Dimensional Case," *Transactions of ASME, Journal of Applied Mechanics*, Vol. 26, No. 3, Sept. 1959, pp. 415-421.
- <sup>7</sup>Mead, D. J. and Markus, S., "The Forced Vibration of a Three-Layer, Damped Sandwich Beam with Arbitrary Boundary Conditions," *Journal of Sound and Vibration*, Vol. 10, No. 2, Aug. 1969, pp. 163-175.
- <sup>8</sup>Di Taranto, R. A., "Theory of Vibratory Bending for Elastic and Viscoelastic Layered Finite-Length Beams," *Transactions of ASME, Journal of Applied Mechanics*, Vol. 32, No. 4, Dec. 1965, pp. 881-892.
- <sup>9</sup>Hashin, Z., "Plane Anisotropic Beams," *Transactions of ASME, Journal of Applied Mechanics*, Vol. 34, No. 2, June 1967, pp. 257-262.
- <sup>10</sup>Krajcinovic, D., "Vibrations of Laminated Beams," AIAA Paper 72-399, April 1972.
- <sup>11</sup>Kimel, W. R., Raville, M. E., Kirmser, P. G., and Patel, M. P., "Natural Frequencies of Vibration of Simply Supported Sandwich

Beams," *Proceedings of the Fourth Midwestern Conference on Solid Mechanics*, Univ. of Texas Press, Austin, TX, 1959, pp. 441-456.

<sup>12</sup>Raville, M. E., Ueng, E.-S., and Lei, M.-M., "Natural Frequencies of Vibration of Fixed-Fixed Sandwich Beams," *Transactions of ASME, Journal of Applied Mechanics*, Vol. 28, No. 3, Sept. 1961, pp. 376-381.

<sup>13</sup>James, W. L., "Calculation of Vibration Damping in Sandwich Construction from Damping Properties of the Cores and Facings," Forest Products Lab., Madison, WI, Rept. No. 1888, Dec. 1962.

<sup>14</sup>Glaser, A. R., "The Vibration of Sandwich Beams," *Developments in Mechanics*, Vol. 1, Plenum, New York, 1961, pp. 228-238.

<sup>15</sup>Clary, R. R. and Leadbetter, S. A., *An Analytical and Experimental Investigation of the Natural Frequencies of Uniform Rectangular-Cross-Section Free-Free Sandwich Beams*, NASA TN-D-1967, Oct. 1963.

<sup>16</sup>Bert, C. W., Wilkins, D. J., Jr., and Crisman, W. C., "Damping in Sandwich Beams with Shear-Flexible Cores," *Transactions of ASME, Journal of Engineering for Industry*, Vol. 89, No. 4, Nov. 1967, pp. 662-670.

<sup>17</sup>Lo, H. and Renbarger, J. L., "Bending Vibrations of a Rotating Beam," *Proceedings of the First U. S. National Congress of Applied Mechanics*, Illinois Institute of Technology, Chicago, IL, 1951, pp. 75-79.

<sup>18</sup>Boyce, W. E., Di Prima, R. C., and Handelman, G. H., "Vibrations of Rotating Beams of Constant Section," *Proceedings of the Second U.S. National Congress of Applied Mechanics*, American Society of Mechanical Engineers, New York, 1954, pp. 165-172.

<sup>19</sup>Tomar, J. S. and Jain, R., "Thermal Effect on the Frequencies of a Rotating Wedge-Shape Beam," *AIAA Journal*, Vol. 22, June 1984, pp. 848-850.

<sup>20</sup>Hoa, S. V., "Vibration of a Rotating Beam with Tip Mass," *Journal of Sound and Vibration*, Vol. 67, No. 3, Dec. 1979, pp. 369-381.

<sup>21</sup>Laurenson, R. M., "Influence of Mass Representation on the Equation of Motion for Rotating Structures," *AIAA Journal*, Vol. 23, Dec. 1985, pp. 1995-1998.

<sup>22</sup>Brunelle, E. J., "Stress Redistribution and Instability of Rotating Beams and Disks," *AIAA Journal*, Vol. 9, April 1971, pp. 758-759.

<sup>23</sup>Brunelle, E. J., "The Super Flywheel: A Second Look," *Transactions of ASME, Journal of Engineering Materials and Technology*, Vol. 95, Jan. 1973, pp. 63-65.

<sup>24</sup>Bishop, K. E., "Discussion of the Super Flywheel: A Second Look," *Transactions of ASME, Journal of Engineering Materials and Technology*, Vol. 95, July 1973, pp. 195-196.

<sup>25</sup>Bert, C. W., "Perturbation Analysis of Quasi-Static Behavior of Brush-Type Super Flywheels," *Mechanics Research Communications*, Vol. 3, No. 4, 1976, pp. 237-243.

<sup>26</sup>Shigley, J. E., *Mechanical Engineering Design*, 3rd ed., McGraw-Hill, New York, 1977, p. 41.

<sup>27</sup>Timoshenko, S. and Young, D. H., *Elements of Strength of Materials*, 5th ed., Van Nostrand, Princeton, NJ, 1968, p. 199.

<sup>28</sup>Cowper, G. R., "The Shear Coefficient in Timoshenko's Beam Theory," *Journal of Applied Mechanics*, Vol. 33, June 1966, pp. 335-340.

## Recommended Reading from the AIAA Progress in Astronautics and Aeronautics Series . . .



# Opportunities for Academic Research in a Low-Gravity Environment

George A. Hazelrigg and Joseph M. Reynolds, editors

The space environment provides unique characteristics for the conduct of scientific and engineering research. This text covers research in low-gravity environments and in vacuum down to  $10^{-15}$  Torr; high resolution measurements of critical phenomena such as the lambda transition in helium; tests for the equivalence principle between gravitational and inertial mass; techniques for growing crystals in space—melt, float-zone, solution, and vapor growth—such as electro-optical and biological (protein) crystals; metals and alloys in low gravity; levitation methods and containerless processing in low gravity, including flame propagation and extinction, radiative ignition, and heterogeneous processing in auto-ignition; and the disciplines of fluid dynamics, over a wide range of topics—transport phenomena, large-scale fluid dynamic modeling, and surface-tension phenomena. Addressed mainly to research engineers and applied scientists, the book advances new ideas for scientific research, and it reviews facilities and current tests.

TO ORDER: Write AIAA Order Department,  
370 L'Enfant Promenade, S.W., Washington, DC 20024  
Please include postage and handling fee of \$4.50 with all orders.  
California and D.C. residents must add 6% sales tax. All foreign orders  
must be prepaid. Please allow 4-6 weeks for delivery. Prices are subject  
to change without notice.

1986 340 pp., illus. Hardback  
ISBN 0-930403-18-5  
AIAA Members \$59.95  
Nonmembers \$84.95  
Order Number V-108